Base Metal Microstructural Considerations for Aluminum Finishing

Jude M. Runge, C.J. Saporito Plating Company, Cicero, IL

Material tested and found to be conforming to design specifications may sometimes exhibit finish deficiencies after anodizing in a well controlled process, while different lots of conforming material (same alloy and temper) finish well through this same process. The cause of this behavior is found in the overlooked characteristic of microstructure. This paper examines the relationship between temper designations, microstructure, and the precipitation hardening process and the ability to mask overaged conditions of aluminum, rendering it not readily processable by standard anodizing.

For more information, contact:
Aaron J. Pomis
Jude M. Runge, Ph.D.
C.J. Saporito Plating Company
3119 South Austin Avenue
Cicero, IL 60804

Phone: 708-222-5300
FAX: 708-780-0741
ajpcjslab@aol.com
jrmcjslab@aol.com

Introduction

Alloy Selection for Light Metal Components

Aluminum, Magnesium, Titanium, and Beryllium are classified "light metals" as they are frequently used to reduce the weight of components and structures. The property of "lightness" is related to the relative density of the material, 2.7 and 1.7, for aluminum and magnesium respectively. Upon Comparison to the older structural metals; 7.9 for iron, and 8.9 for copper, it is easy to see why the "light metals" are the preferred materials in the transportation industry, most especially in the aerospace and defense industries where minimizing payload weight can reduce fuel consumption and decrease flight time, which are important economic considerations.

In addition to the low density, aluminum exhibits a high strength to weight ratio, high corrosion resistance, and, electrical and thermal conductivities. Aluminum is also readily machinable and its by-products are not toxic or pyroforic like those of beryllium and magnesium. It is also not as expensive as Titanium. Aluminum, therefore has become the material of choice for certain applications in the electronics and communication industries, specifically in thermal products: chassis, housings, and heat sinks, in which all of the favorable characteristics can be put into use. Table 1 compares the properties of the "light metals" to those utilized previously for similar applications.

The source for Aluminum's inherent corrosion resistance is in its high surface reactivity. Aluminum oxidizes readily, producing a stable passive film. The thickness and uniformity of the film can vary, depending upon the conditions for its information. Anodizing is one of the most common processes utilized today which imparts and controls a uniform oxide file of sufficient thickness to enhance corrosion resistance and maintain thermal conductivity. Both cast and wrought products can be anodized.

In the electronics and communications industries, cast aluminum is sometimes used for connector bodies and housings; however, most assemblies utilize the sheet and/or extruded product. Since the focus of this paper is on the use of aluminum in thermal products (heat sinks), wrought products only will be considered.

The Significance of Wrought Aluminum Alloy and Temper Designations

Each wrought alloy has a four-digit number of which the first digit is assigned on the basis of the major alloying element(s). The 1XXX series alloys are essentially unalloyed aluminum, with 99% aluminum minimum. The 2XXX series alloys contain copper as their major alloying element. The 3XXX series, manganese, 4XXX series, silicon, 5XXX series magnesium, 6XXX series, magnesium and silicon, and the 7XXX series, zinc. The remaining digits indicate the variations in the trace element constituents, and for the 1XXX series alone, minimum aluminum purity. Each class of alloys behaves differently, with compositions and structure dictating the working characteristics and subsequent properties. Copper is normally added for strength, chromium to offset the loss of corrosion resistance because of copper additions. Iron is added as a dispersion-hardening agent. Magnesium enhances corrosion resistance and silicon, strength.

As cast, aluminum is a soft metal. The high strength to weigh ratio touted earlier as a favorable characteristic is achieved in certain aluminum alloys through its significant response to precipitation, which occurs during age hardening. These alloys have 2XXX, 6XXX, and 7XXX series designations followed by the letter T with corresponding digits representing the heat treatment (tempering) sequence. Characteristic hardnesses are obtained through controlled tempering sequences by virtue of precipitation, making temper a specifiable attribute for engineering design. Other alloys, classified as non-heat treatable, derive their strength throughout strain hardening (various degrees of cold work). These Alloys are designated 1XXX, 3XXX and 5XXX followed by the letter H with corresponding digits representing the degree of cold work, also a specifiable attribute.

The case study, which follows, deals specifically with aluminum a lot 6061 T6. The 6XXX series alloys are unique in that they incorporate two major alloying constituents, magnesium and silicon. The T6 temper indicates the material has been solution treated and artificially aged to a stable hardness of 73HB.

Review of the binary phase diagrams for the system; Al-Mg, Al-Si and Mg-Si (see figure nos. 1 and 2) [1], as well as literature dealing with the 6XXX series alloys, indicates the major solute intermetallic phase that forms is Mg_2Si. Balanced

amounts of magnesium and silicon are added to for quasi-binary Al – Mg_2Si alloys (see figure nos. 3 and 4) [2,3]. These alloys comprise the majority of aluminum extrusions and exhibit good weldability corrosion resistance, accept coatings well, and are immune to stress corrosions cracking. Alloy 6061 (Al – 1Mg-0.6Si) contains 0.25% copper to improve strength and 0.2% chromium to offset any deleterious effects the copper may have on corrosion resistance. Like all of the 6XXX series alloys, the strength of 6061 is developed through precipitation (age) hardening.

Mechanism for Precipitation in Age Hardening Alloys

Precipitation can best be described as decomposition of a supersaturated solid solution into its parent phase and excess rejected solute atoms. The rejected solute atoms agglomerate to form a small crystal of their own, perhaps with a few solvent atoms dissolved in it, or react with some of the solvent atoms to form a phase of a crystal structure different from that of either pure metal (i.e. an intermetallic compound). The agglomerate is the precipitate. It enhances the hardness of the soft matrix by increasing local stress within the microstructure by restricting, "pinning" dislocation movement across the crystal.

Precipitation hardenable alloys are characterized by phase diagrams such as figure 4, the quasi-binary phase diagram for Al-Mg_2Si. The precipitation hardening process can be generalized as follows:

Solution treatment at a relatively high temperature within the single-phase region to dissolve the alloying elements. Rapid cooling or quenching, usually to room temperature, to obtain a supersaturated solid solution of these elements in the aluminum matrix. Controlled decomposition of the supersaturated solid solution to form a finely dispersed precipitate, by aging for appropriate times at one and sometimes two intermediate temperatures.

The precipitation sequence involves the nucleation, growth, and development of the equilibrium phase. Since precipitation is from a supersaturated solution, the driving force for the formation of the equilibrium phase is large, and is dependant upon the amount of undercooling achieved through quenching (the larger the undercooling, the larger the driving force). Nucleation is heterogeneous within the supersaturated solution because of the presence of quenched-in vacancies, dislocations, and grain boundaries. The driving force for the heterogeneous nucleation of precipitates is therefore presented as the change in volume free energy due to strain plus the surface free energy of the developing precipitates less the free energy of the defects which lower the free energy by providing surfaces for nucleation.

$$G_{het} = -V(\Delta G_v - \Delta G_s) + \gamma_A - \Delta G_d \qquad (1)$$

The process involves the transition through intermediate phases originating with the nucleation of Guinier-Preston (GP) zones. GP zones are ordered, solute-rich clusters of atoms, which retain the structure of matrix and are coherent with it. Because of their coherent nature, they have a lower interfacial energy than the equilibrium phase. Mondolfo[2] indicated for the 6XXX series alloys that the GP zones are spherical, which also reduces the lattice misfit strain. This reduces the barrier to nucleation for the GP zones and they form prior to the intermediate phases which simultaneously: a) have higher interfacial energies and b) require additional energy for solute interdiffusion. This latter requirement is more prevalent in the 6XXX series alloys than in any other aluminum alloy as they require the activation energy to form the equilibrium intermetallic phase Mg_2Si.

After the formation of the spherical GP zones, the intermediate phases precipitate. For the 6XXX series alloys, the precipitation sequence leading to the equilibrium phase, Al – Mg_2Si, is preceded by β″ and β′. In describing the precipitation sequence, Mondolfo indicated that the GP zones elongate in the [100] direction. The intermediate phase, β″, has a monoclinic structure and a needle shape. The structure contains a large number of vacancies and the exerts a compressive force on the matrix. The corresponding stress developed through this force increases the hardness of the alloy.

The β″ needles grow to become β′ rods. β′ is semicoherent with the matrix and has a cubic or hexagonal lattice. The departure from coherency increases the compressive force on the matrix, increasing the hardness of the alloy. Peak hardness is reached just before the Mg_2Si platelets (equilibrium phase) form. The equilibrium phase nucleates at the β′ – matrix interface and grows at the expense of β′. A schematic of the precipitation sequence for the 6XXX alloys is presented as figure no. 5.

The activation energy for the formation of GP zones was reported as 0.37 eV; for precipitation, 0.9 eV. Heat evolution corresponding to the formation of the various intermediate phases was also reported. These trends show the intermediate phases that occur during precipitation rather than direct transformation to the equilibrium phase are the result of the lower activation energy barriers per each step. Transformation stops when the minimum free energy equilibrium state of Mg_2Si is reached. See figure no. 6.

The property changes which occur during precipitation hardening and the time-temperature transformation curves for the 6XXX series aluminum alloys are presented as figure no. 7. A definite increase in hardness can be related to the nucleation of the GP zones (A) and the progressive precipitation of the needles to rods (A-B), and rods to platelets (B-C). A decrease in hardness is noted after the formation of the equilibrium phase. Since the increase in hardness is related to the growth of the precipitate phase into the equilibrium phase, and since transformation ceases upon formation of the equilibrium phase, the decrease in hardness must be related to the continued growth (not transformation) of the equilibrium phase.

Precipitate Coarsening

Although completion of the precipitation to the equilibrium phase achieves the minimum free energy of the transformation, instability within the matrix persists because the total interfacial free energy is not at a minimum. Therefore, the high density of a smaller equilibrium precipitates from the initial transformation will continue to coarsen into a lower density of larger equilibrium precipitates to minimize the total interfacial area. The precipitate coarsening produces the decrease in hardness noted in figure 7. Dislocation pinning effectiveness decreases with the decrease in precipitate population. For the precipitation hardenable aluminum alloys, precipitate coarsening will also decrease the corrosion resistance and increase its susceptibility to chemical attack because of increased capillarity at the precipitate-matrix interface.

Because of the differences in the time of nucleation and rate of growth of the precipitates, a tempered specimen will exhibit a range of particle sizes. Although precipitates within the tempered specimen are at the same temperature and have identical structures and compositions, they have different chemical potentials because of their different sizes. The solute concentration gradient in the matrix adjacent to a precipitate will increase as the radius of curvature decreases. This is expressed in Thomson's equation,

$$(\mu_i)_{r'} - (\mu_i)_{r''} = V_i 2\gamma (1/r' - 1/r'') \qquad (2)$$

and the effect is known as Ostwald ripening. The higher chemical potential in the smaller precipitates causes diffusion in the direction of the largest precipitates, away from the smaller precipitates. Therefore, the small precipitates shrink and disappear, "ripening" the large precipitates. Furthermore, the inverse relationship between the surface energy and the precipitate radius shows the relative instability of the smaller precipitates and the driving force for the particle coarsening. Because the reaction is diffusion controlled, the rate of coarsening will increase with increasing temperature. See figure no. 8.

Anodizing Aluminum

Anodizing is the common designation for the anodic oxidation of certain metals to form stable oxide films on their surfaces. [9] Films of various hardnesses and thicknesses can be produced to serve varying purposes by adjusting process parameters. Most commonly, the anodizing process is utilized to produce decorative finishes, to increase the corrosion or abrasion resistance of the substrate metal, or to provide an adherent interface for subsequent coatings. For the case study that follows, the parameters documented for producing the latter two qualities will be considered.

Research has shown that anodic films are dual phase aluminum oxide, i.e. Al_2O_3. The dual structure consists of a thin, nonporous inner oxide adjacent to the base metal (also called the barrier layer) and a thick porous outer oxide. The outer porous oxide has a columnar cell structure (see figure no. 9). The microstructure and thickness of the layers depend upon the parameters of the anodizing process, specifically; time, temperature, bath composition, and formation voltage. The outer porous film is composed of partially hydrated alumina and the barrier later is dense alumina.

Sulfuric acid solutions, 5 – 25% by volume, are the most widely used anodizing electrolytes. Anodic films utilized for subsequent coating applications are usually produced from a 10% sulfuric acid electrolyte. The bath is usually operated at temperatures of 20 – 25 °C, a current density of 1.5 amps/dm^2, and a bath voltage of 10 – 25V. The films

produced range in thickness from 16 – 30 microns. Thicker and more porous coatings which exhibit higher hardness, are produced by increasing the bath voltage and current density and decreasing the operating temperature. It is well documented that the anodic film can retain electrolyte in the form of residual sulfonic acid groups.[9,10]

The inherent porous nature of the outer layer of the anodic film requires the film be sealed to effect a protective coating. The mechanism of sealing is not fully understood but is thought to involve conversion of the amorphous oxide of the pores into alpha-alumina monohydrate, this conversion being accompanied by a change in volume. The volume change seals the oxide film by "plugging" the pores so that the anodic film becomes impermeable and its protective capability for the substrate metal is enhanced. Various types of sealants have been developed to increase corrosion resistance, dye, and/or ensure good lubrication of wear surfaces. Most simplistically, boiling water is utilized. Most commonly, nickel acetate is utilized.

Case Study: The Effects of Microstructure on the Anodizing Process

Several samples of black anodized alloy 6061 T6 aluminum heat sinks were submitted to determine the nature and cause for a surface condition identified as "smut". See Photos nos. 1 and 2.

The samples were subjected to chemical analysis and hardness testing and found to be in compliance with the material specifications. Scrutiny of the anodizing process found nothing out of the ordinary and all aspects of the process found under control. Furthermore, other material similarly tested and found compliant from different tempering lots processed well.

Comparative analysis of the microstructures at the coated surface and within the bulk of heat sinks which exhibited the "smut" condition and those that did not determined the following results. The samples which exhibited the "smut" were determined to have a microstructure with coarse, intergranular precipitates. Those which processed well exhibited comparable grain sizes but exhibited finer, more well dispersed precipitates. See Photographs nos. 3 – 6.

The determined similarities in base metal hardness, differences in microstructure, and referral to figure no. 6 indicated the base aluminum had been overawed during heat treating to a point where identical hardness to a T6 temper was achieved. Unfortunately, exposure of the coarser microstructure to the chemicals and potential of the anodizing process produced large intergranular pits in the aluminum surface. The columnar microstructure of the anodized film could not properly form across these pits, which produced a discontinuous structure. The discontinuous structure retained anodizing solution which wept out as the component dried, producing the observed "smut"

Recommendations were made to the coater of this product to return any unprocessed 6061 "T6" material from the overaged lot for resolution treatment and proper tempering. Unfortunately, none existed. However, a routine analysis program was begun to verify microstructure of the extrusions prior to coating as well as the chemistry and hardness.

Conclusion

The light metals, especially aluminum, fill an important niche in the transportation, electronics, and communications industries. Many of the desirable characteristics of the light metals are obtained through heat treatment. As with any material, it is necessary that subsequent processing be well controlled such that the resultant material characteristics derived through that process is what is desired. Understanding the metallurgical aspects of the materials history, for this case, heat treatment and finishing, can 1) optimize finish product and quality and 2) expedite failure analysis in the event of a defect.

Based upon the information presented in this paper, one can see two metallurgical phenomena must be considered for optimization of the aluminum base metal microstructure. They are: the changes which occur due to the progressive transformations during the precipitation sequence, and the changes which can occur to the microstructure after the equilibrium phase has been achieved though precipitation and transformations have stopped. It is clear that control of the time and temperature of the thermal processing of aluminum alloys is necessary to assure quality in the finished product.
JRM 30 April 1995

BIBLIOGRAPHY

ASM International Metals Handbook, Tenth Edition, Volume 3, Alloy Phase Diagrams.

Mondolfo, L.F., Aluminum Alloys, Structure & Properties, Butterworth &Co., London, 1976.

Polmear, I.J., Light alloys, Metallurgy of the Light Metals, American Society for Metals, 1982.

Brooks, Charlie R., Heat Treatment, Structure and Properties of Nonferrous Alloys, American Society for Metals, 1982.

Porter, D.A., and Easterling, K.E., Phase Transformations in Metals and Alloys, Second Edition, Chapman and Hall, 1992

Reed-Hill, Robert E., Physical Metallurgy Principles, Second Edition, D. Van Nostrand Company, New York, 1973.

Lupis, C.H.P., Chemical Thermodynamics of Materials, North-Holland, New York, 1983

Murr, Lawrence E., Interfacial Phenomena in Metals and Alloys, Addison-Wesley Publishing Co., 1975.

Von Fraunhofer, J.A., Basic Metal Finishing, Chemical Publishing, New York, 1976.

ASM International Metals Handbook, Ninth Edition, Vol. 5, Surface Cleaning, Finishing, and Coating, 1985.

Table 1 Some physical properties of pure metals (from Smithells, C. J., *Metals Reference Book*, 5th edition, Butterworths, London, 1976)

Property	Unit	Al	Mg	Ti	Be	Fe	Cu
Melting point	°C	660	650	1678	1287	1535	1083
Relative density (d)		2.70	1.74	4.51	1.85	7.87	8.96
Elastic modulus (E)	GPa	70	45	120	295	211	130
Specific modulus (E/d)		26	26	26	160	27	14
Mean specific heat 0–100°C	J kg^{-1} K^{-1}	917	1038	528	2052	456	386
Thermal conductivity 20–100°C	W m^{-1} K^{-1}	238	156	26	194	78	397
Coefficient of thermal expansion O–100°C	10^{-6} K^{-1}	23.5	26.0	8.9	12.0	12.1	17.0
Electrical resistivity at 20°C	μ ohm cm^{-1}	2.67	4.2	54	3.3	10.1	1.69

Note: Conversion factors for SI and Imperial units are given In the Appendix

Fig. 1: Binary Phase Diagrams for 6XXX series Al alloys

Al-Mg

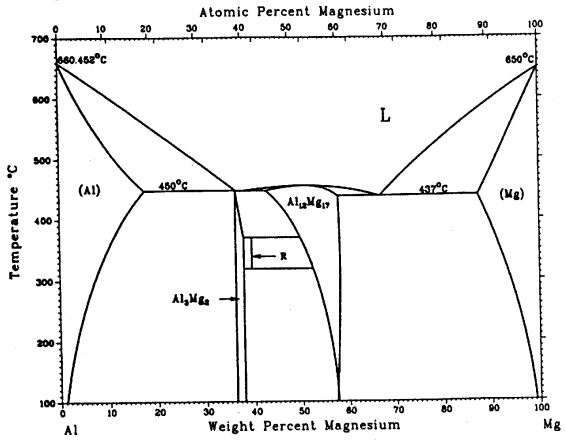

J.L. Murray, 1988

Phase	Composition, wt% Mg	Pearson symbol	Space group
(Al)	0 to 17.1	*cF*4	$Fm\bar{3}m$
$\beta(Al_3Mg_2)$	36.1 to 37.8	*cF*1168	$Fd\bar{3}m$
R	39	*hR*53	$R\bar{3}$
$\gamma(Al_{12}Mg_{17})$	42 to 58.0	*cI*58	$I\bar{4}3m$
(Mg)	87.1 to 100	*hP*2	$P6_3/mmc$
Metastable phases			
Al_2Mg	31.0	*tI*24	$I4_1/amd$
γ'	38 to 56.2	(a)	...

(a) Tetragonal

Al-Si

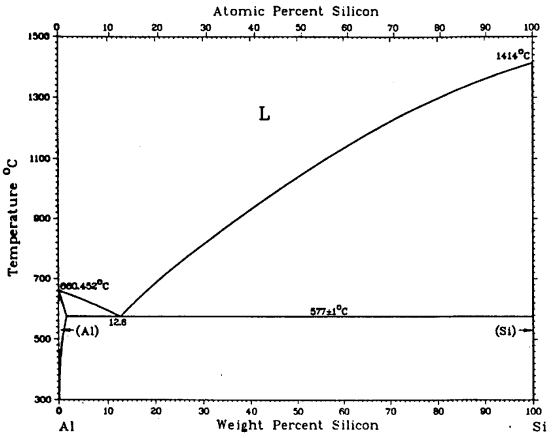

J.L. Murray and A.A. McAlister, 1984

Phase	Composition, wt% Si	Pearson symbol	Space group
(Al)	0 to 1.6	*cF*4	$Fm\bar{3}m$
(Si)	99.985 to 100	*cF*8	$Fd\bar{3}m$

Mg-Si

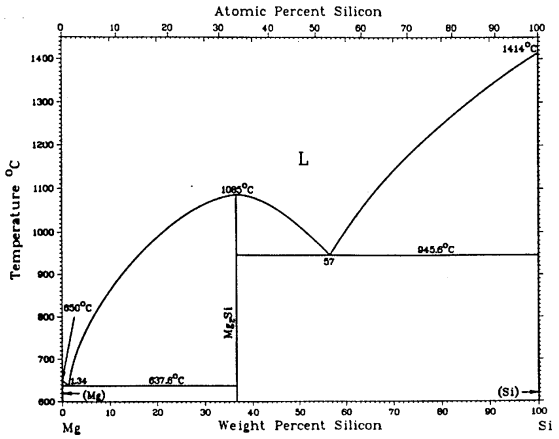

A.A. Nayeb-Hashemi and J.B. Clark, 1988

Phase	Composition, wt% Si	Pearson symbol	Space group
(Mg)	~0	*hP*2	$P6_3/mmc$
Mg_2Si	36.61	*cF*12	$Fm\bar{3}m$
(Si)	~100	*cF*8	$Fd\bar{3}m$
High-pressure phases			
Mg_2Si(a)	36.61	...	...
SiII	100	...	...

(a) Above ~2.5 GPa and 900 °C, it forms a hexagonal structure.

Fig. 2: Ternary Phase Diagrams for 6XXX series Al alloys

Al-Mg-Si liquidus projection [73Wil]

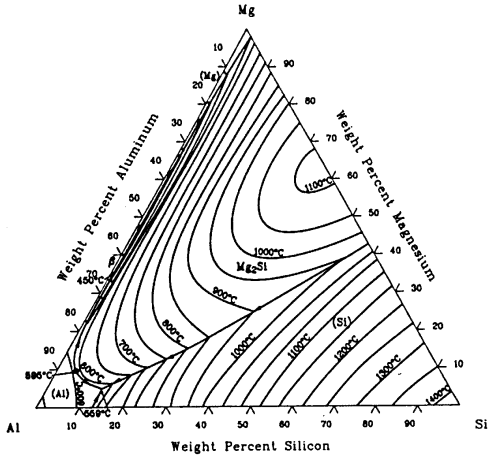

Al-Mg-Si solidus projection [73Wil]

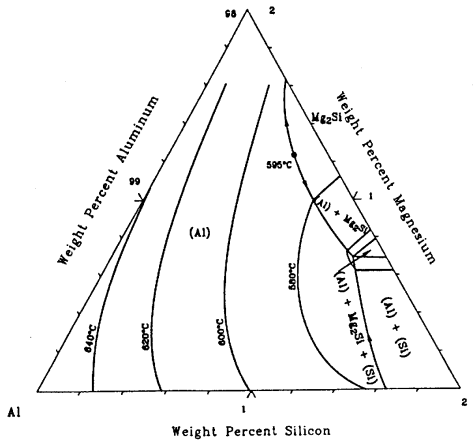

Al-Mg-Si solvus projection [73Wil]

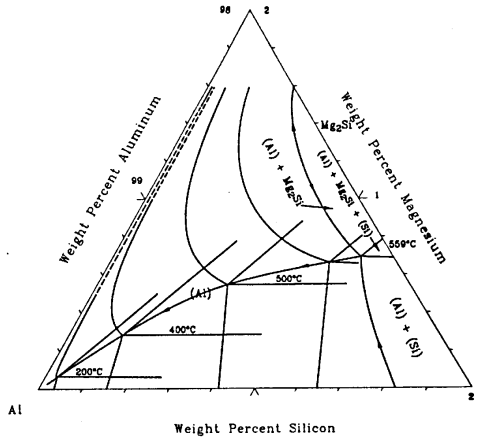

Al-Mg-Si isothermal section at 800 °C [88Rok]

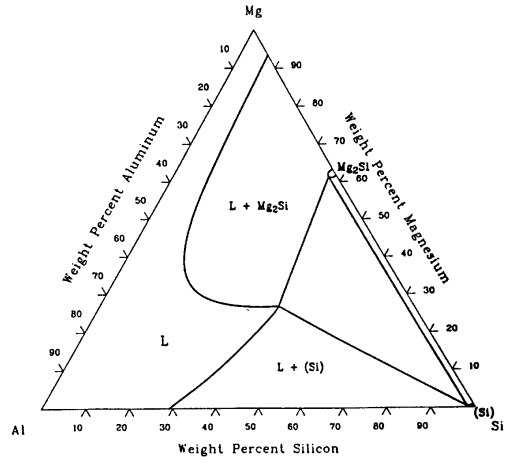

Al-Mg-Si isothermal section at 430 °C [88Rok]

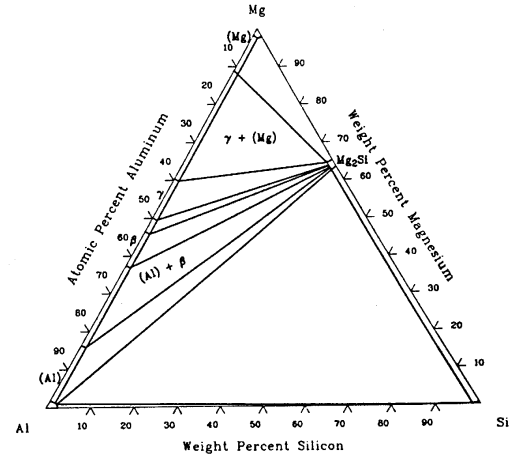

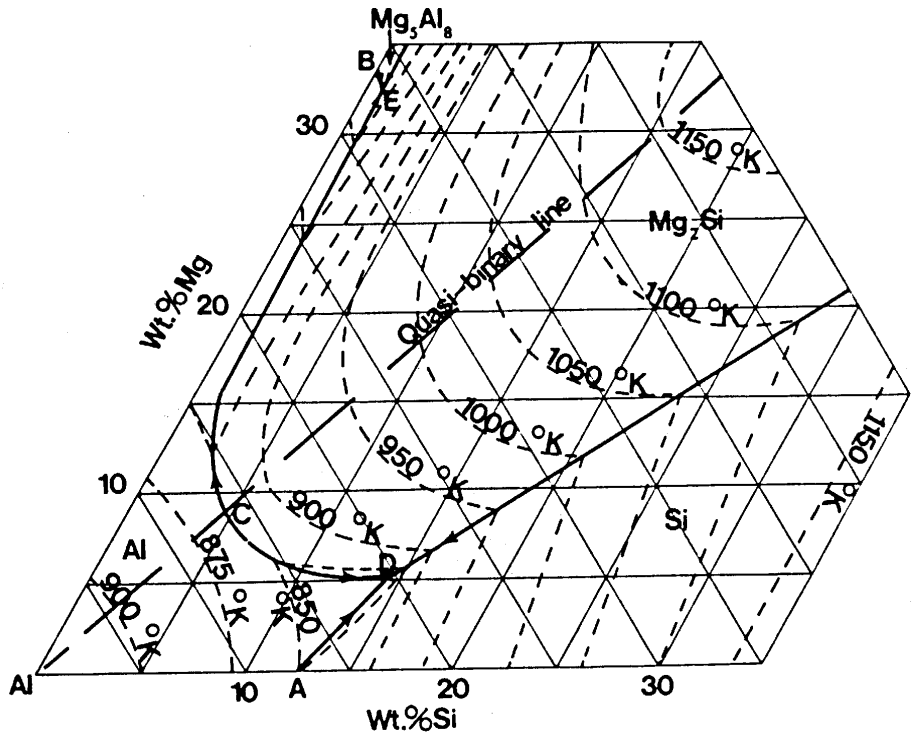

(a)

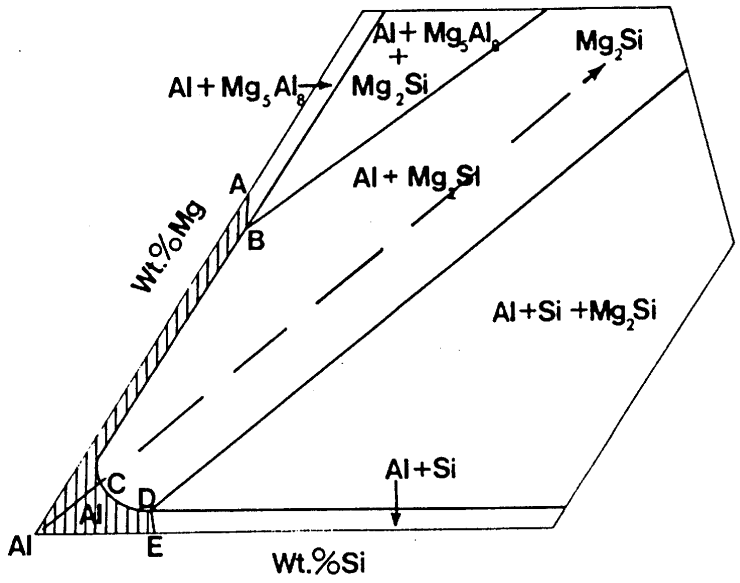

(b)

Figure 3. Aluminum corner of the aluminum–magnesium–silicon diagram

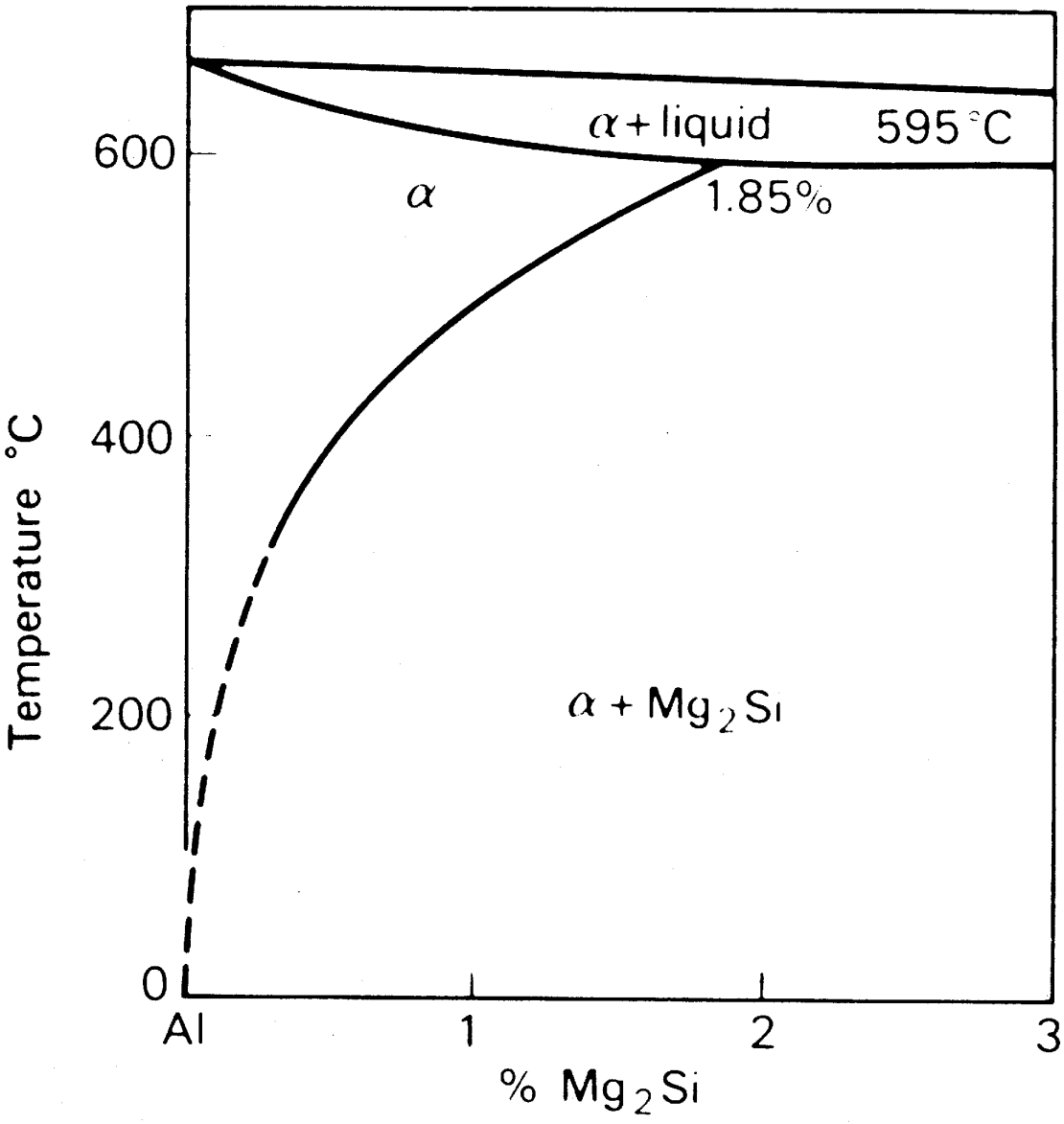

Fig. 4 Pseudo-binary phase diagram for Al-Mg_2Si

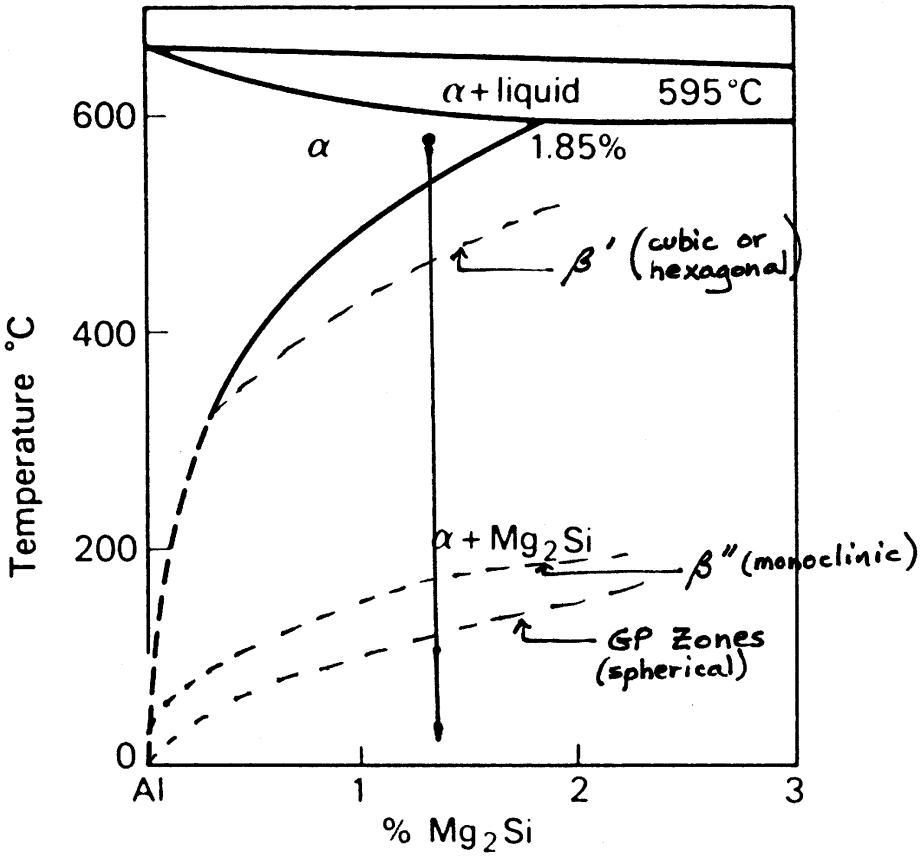

Fig. 5 Pseudo-binary phase diagram for Al-Mg_2Si

Precipitation sequence :

GPZ (spheres) → β" (needles) → β' (rods) → Mg_2Si (platelets)

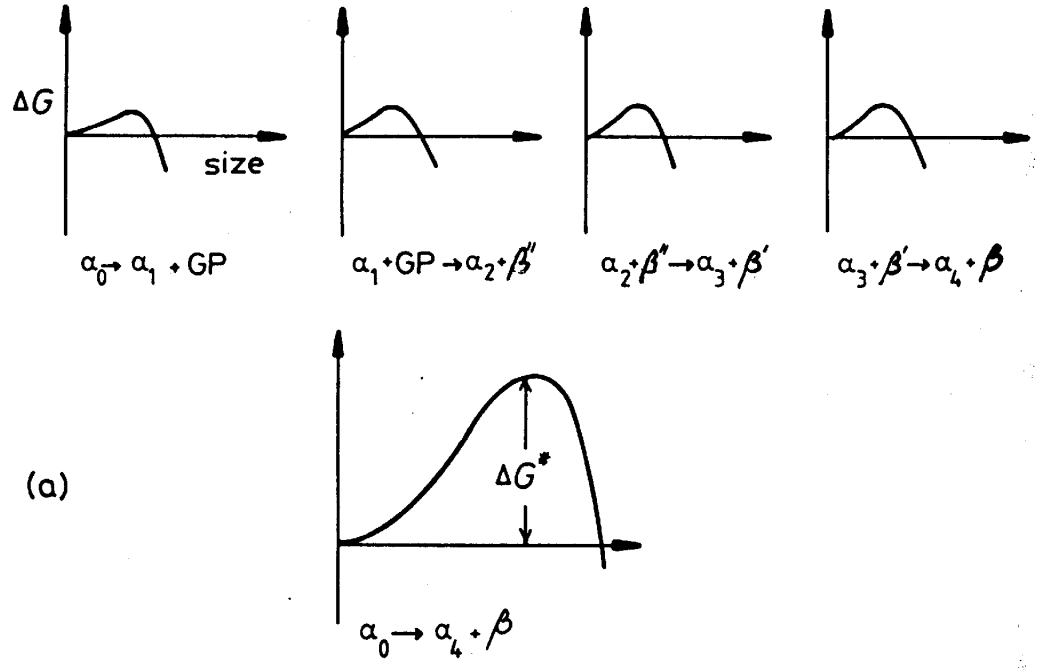

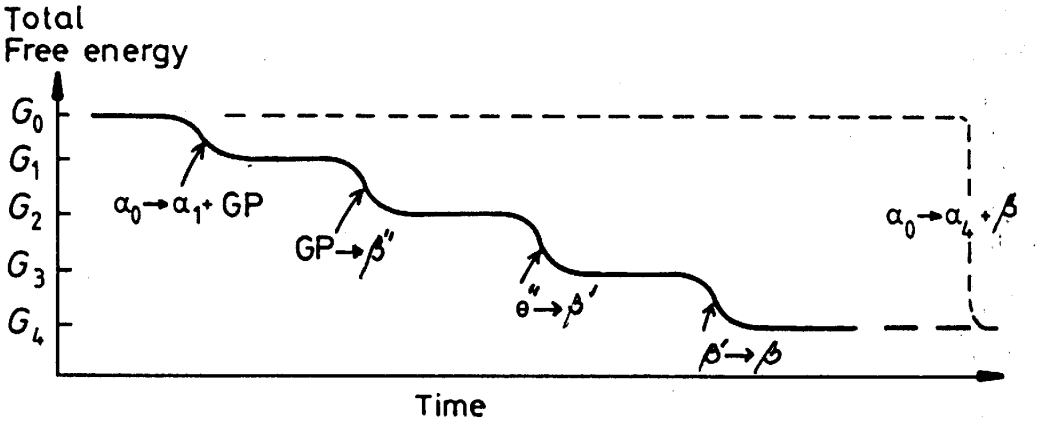

(b)

Fig. 6 (a) The activation energy barrier to the formation of each transition phase is very small in comparison to the barrier against the direct precipitation of the equilibrium phase. (b) Schematic diagram showing the total free energy of the alloy v. time.

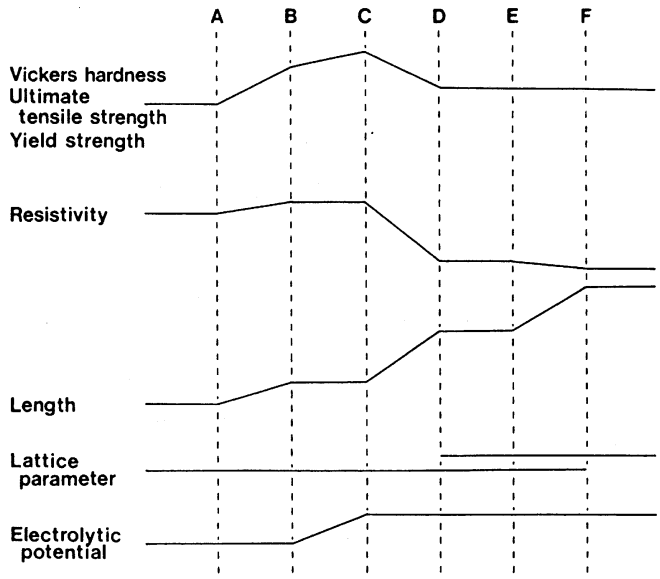

Fig. 7a. Schematic properties changes during aging of aluminum–magnesium silicide alloys

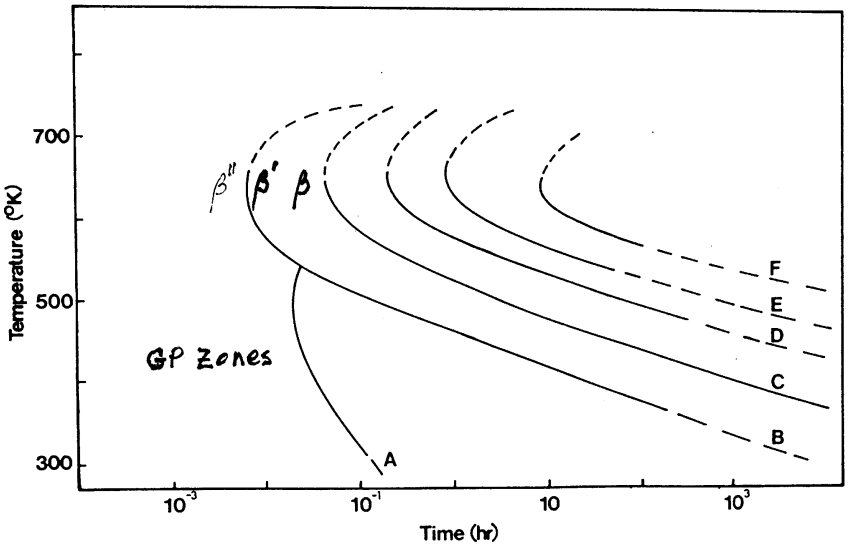

Figure 7b. TTT curves of an alloy with 1.8% Mg_2Si

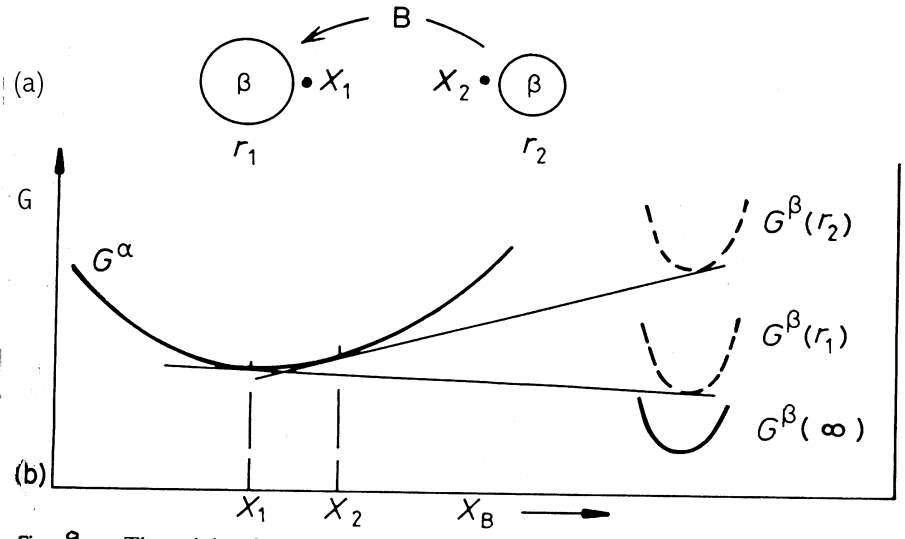

Fig. 8 The origin of particle coarsening. β with a small radius of curvature (r_2) has a higher molar free energy than β with a large radius of curvature (r_1). The concentration of solute is therefore highest outside the smallest particles.

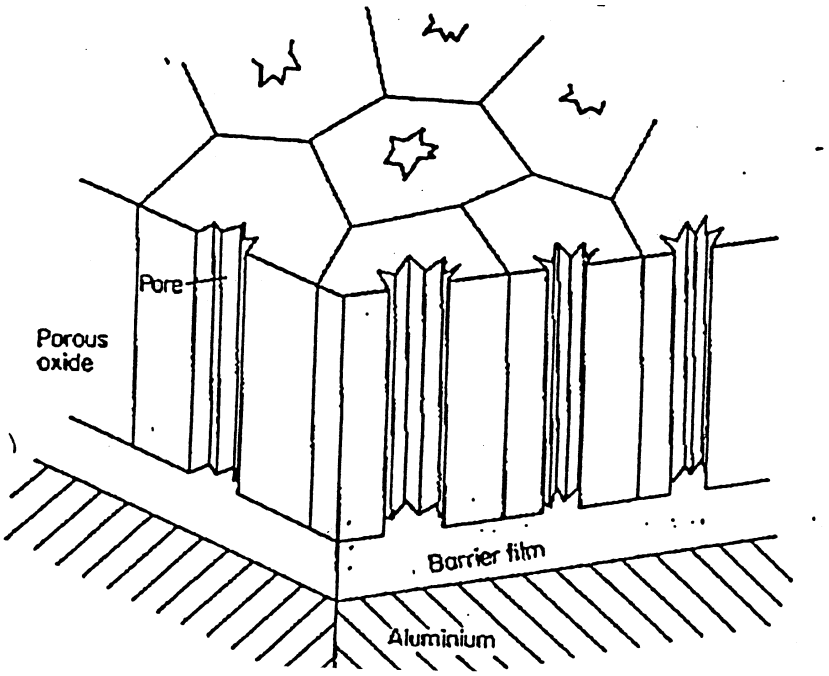

Figure 9: Schematic Structure of Anodized Film on Aluminum

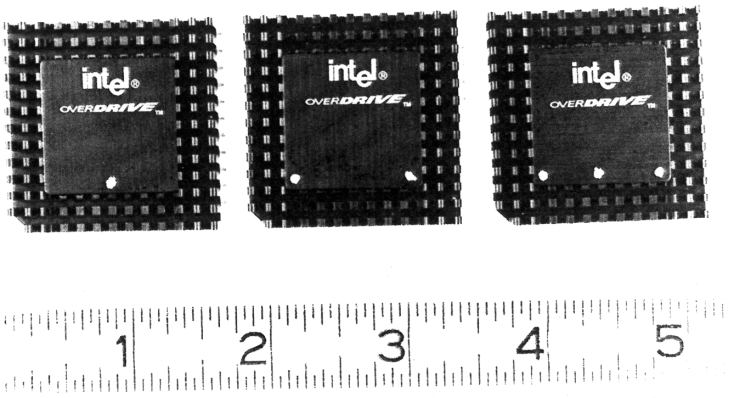

Photo 1:

Documentary photograph of black anodized 6061 aluminum heat sinks.

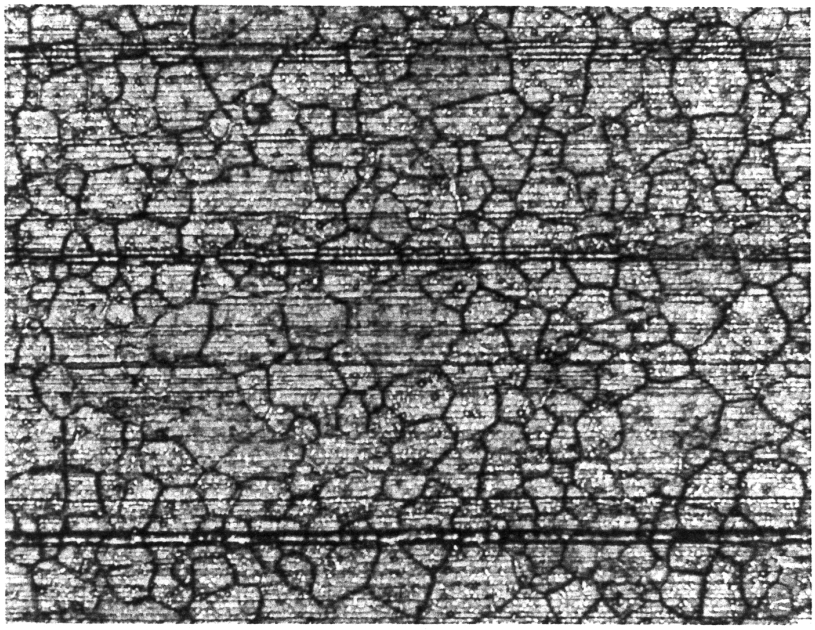

Photo 2

X100 High magnification photomacrograph of the anodized surface Note the heavy grain boundary relief. The film exhibited a "smutty" appearance which was cause for rejection.

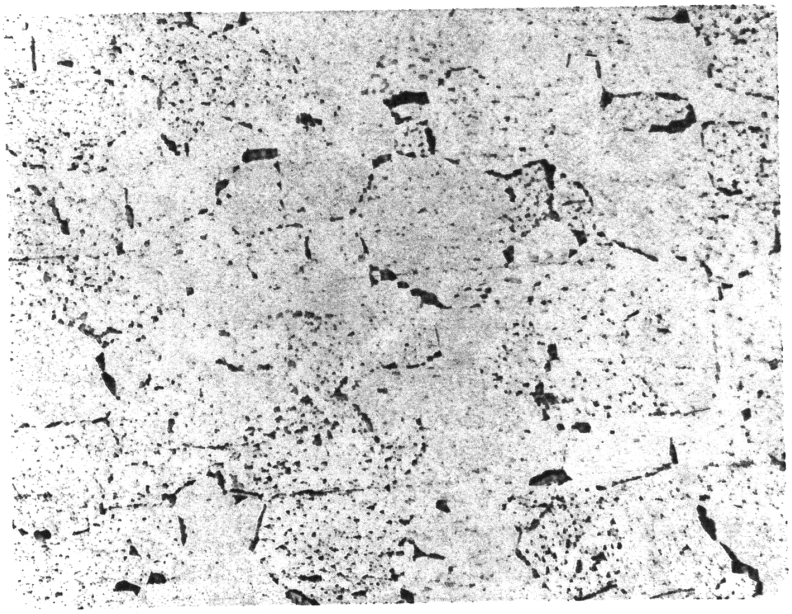

Photo 3

X400 Etchant: Tucker's Reagent

Representative photomicrograph of heat sink microstructure. Note the coarse precipitation at the grain boundaries.

Photo 4

X400 Etchant: Keller's Reagent

Anodized Film on overaged aluminum. Note the lack of fusion within the Boehmitic (columnar) phase of the film. Deep etch pits correspond to areas of coarse precipitate removal.

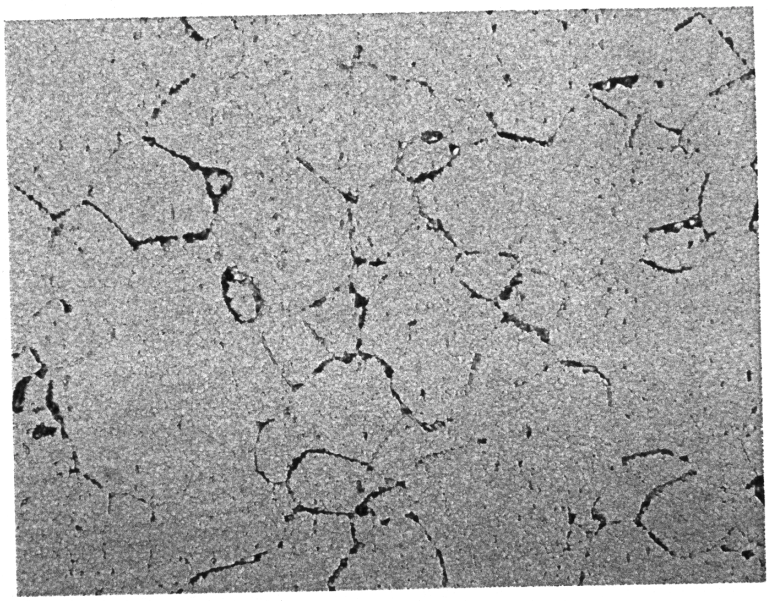

Photo 5

X400 Etchant: Tucker's Reagent

Representative photomicrograph of "good" heat sink microstructure. Note although some coarse precipitation exists at the grain boundaries, the overall microstructure does not exhibit as severe an overaged appearance.

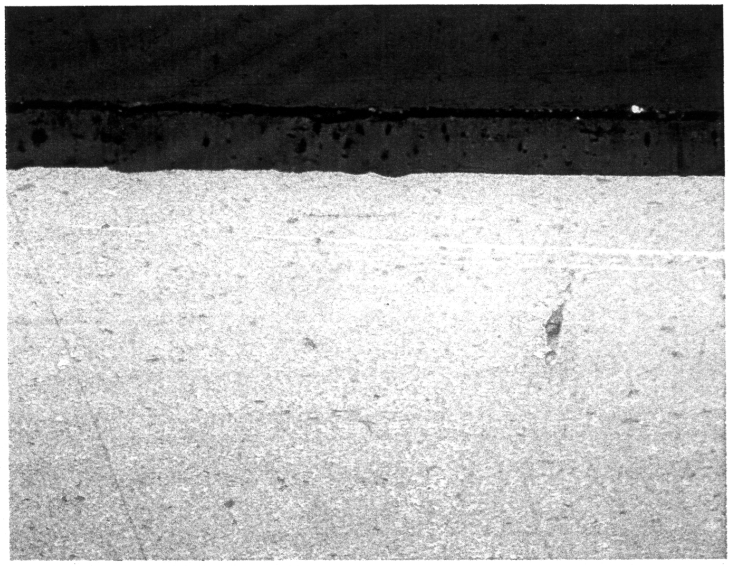

Photo 6

X400 Etchant: Keller's Reagent

Microstructure typical of the anodic film on a "good" heat sink. Note the continuous boehmitic structure as well as minor aluminum surface undulation as the result of chemical attack during coating